MAUSAM, **74**, 1 (January, 2023), 169-176

MAUSAM

DOI : https://doi.org/10.54302/mausam.v74i1.5607
Homepage: https://mausamjournal.imd.gov.in/index.php/MAUSAM

UDC No. 551.577 : 551.509.314 (663)

Statistical modeling of monthly maximum rainfall in Senegal

KOUAKOU INNOCENT N'DRI and SARALEES NADARAJAH*

AIMS Senegal, Mbour-Thies, Senegal

**University of Manchester, Manchester M13 9PL, UK*

(*Received 21 March 2022, Accepted 22 November 2022*)

e mails : kouakou.i.ndri@aims-senegal.org; mbbsssn2@manchester.ac.uk

सार – हम सेनेगल में अधिकतम वर्षा का पहला सांख्यिकीय विश्लेषण प्रस्तुत कर रहे हैं। इसमें सेनेगल में फैले बारह स्टेशनों का डेटा हैं। अधिकतम संभावना की विधि द्वारा सामान्यीकृत चरम मूल्य वितरण को अधिकतम वर्षा के लिए फिट किया गया था। संभाव्यता और विभाजित भूखंडों तथा उचित परीक्षणों की सही स्थिति से पता चला है कि सामान्यीकृत चरम मूल्य वितरण सभी स्टेशनों के लिए पर्याप्त रूप से सही है। अधिकांश स्टेशन वर्षा के महत्वपूर्ण प्रवृत्तियों को प्रदर्शित नहीं करते हैं। इनमें से चार स्टेशनों ने वर्षा में सकारात्मक प्रवृत्ति को प्रदर्शित किया। इसमें प्रत्यंतर स्तर के आकलन दिए गए हैं।

ABSTRACT. We provide the first statistical analysis of maximum rainfall in Senegal. The data are from twelve stations spread across Senegal. The generalized extreme value distribution was fitted to maximum rainfall by the method of maximum likelihood. Probability and quantile plots as well as goodness of fit tests showed that the generalized extreme value distribution provided an adequate fit for all stations. The vast majority of stations do not exhibit significant trends in rainfall. Four of the stations exhibit positive trends in rainfall. Estimates of return levels are given.

Key words – Generalized extreme value distribution, Maximum likelihood,` Return level.

1. Introduction

Nearly 75 per cent of the population in Senegal works in the agricultural sector, which is regularly threatened by inclement weather such as droughts, floods and other climate changes. Extreme rainfall events in Senegal often cause significant damage to agriculture, ecology, infrastructure, injury and loss of life. On the 5th and 6th of September 2020, Dakar, the capital city of Senegal, as well as Kaolack experienced exceptional rainfall. This extreme rainfall event caused flooding and immense damage. Thousands of people were left homeless and hundreds of hectares of farmland were swallowed up by the waters. Also Dakar, Kaolack and Saint-Louis in 1999, 2000, 2001 and Podor in January 2002 experienced serious floods. These floods led to dismantling of houses. Floods in Dakar are a yearly occurrence. Hence, it is important that an assessment is made of the extreme values of rainfall.

The aim of this paper is to provide the first statistical analysis of monthly maximum rainfall in Senegal. We will be able to answer the following questions and more: What are the wettest areas with respect to monthly maximum rainfall? What are the driest areas with respect to monthly maximum rainfall? The answers to these questions and more could lead to actions (for example, increased agricultural production in wet areas and planting of crops withstanding droughts in dry areas) which may be of help to improve the economy of Senegal.

To the best knowledge of the authors, there have been no papers on maximum rainfall in Senegal. However, there have been several papers focusing on rainfall (not maximum rainfall) in Senegal. For example, Negre *et al.* (1988) estimated and monitored rainfall in Senegal by cumulation of the thermal infrared images of the Meteosat satellite; Kakane and Imbernon (1992) estimated rainfall in Senegal using satellite data; Nzeukou and Sauvageot (2002) studied the distribution of rainfall parameters near the coasts of France and Senegal; Thiam and Singh (2002) provided space-time-frequency analysis of rainfall, runoff and temperature in the Casamance River basin, Southern Senegal; Camberlin and Diop (2003) analyzed interannual variability of the onset and cessation dates of the rainy season in Senegal over 1950-1992 using daily rainfall data from thirty four stations; Sambou (2004) performed frequency analysis of daily rainfall in

TABLE 1

Descriptive statistics of monthly maximum rainfall data

Station	Count	Mean	Min	Max	Median	SD	Coeff. of variation	Skewness	Kurtosis
Capskiring	239	105.72	1	1106.14	1.51	175.45	1.660	2.078	1.667
Dakar	239	40.09	1	478.77	1	2.00	80.071	2.773	1.597
Diourbel	213	48.42	1	420.36	104.64	84.37	1.743	2.107	3.077
Kaolack	239	59.45	1	642.62	1	116.82	1.760	2.324	3.253
Kedougou	224	83.61	1	515.09	6.59	136.50	1.397	1.375	2.235
Kolda	220	87.45	1	683.75	1.13	76.95	1.561	1.759	2.437
Linguere	239	39.72	1	446.27	1	76.95	1.937	2.781	2.616
Matam	239	42.57	1	648.95	1	89.30	2.098	3.672	2.250
Podor	239	23.46	1	290.81	1	49.30	2.102	2.934	2.386
Saintlouis	239	30.69	1	365.48	1	57.61	1.877	2.582	1.723
Tambacounda	239	65.95	1	647.42	1.50	102.56	1.555	2.036	2.024
Ziguinchor	239	112.63	1	826.74	1.51	180.69	1.604	1.855	2.986

the Sahelian area; Fall *et al.* (2006a) presented a geographical information systems-based analysis of monthly rainfall (twenty stations) and mean temperature (twelve stations) for 1971 to 1998 in Senegal; Fall *et al.* (2006b) examined climate variability over Senegal and its relationship to global climate using monthly rainfall for twenty stations; Moron *et al.* (2006) examined space-time characteristics of seasonal rainfall predictability in a tropical region by analyzing observed data and model simulations over Senegal; Moron *et al.* (2008a) provided observational analysis of weather types and rainfall over Senegal; Moron *et al.* (2008b) provided downscaling of general circulation model simulations of weather types and rainfall over Senegal; Ndour *et al.* (2012) characterized rainfall variability in Senegalese rural area and analyzed its implications on water resources in the borough of Fimela; Rust *et al.* (2013) produced a weather-type influence map on Senegal precipitation based on a spatial-temporal statistical model; Faye *et al.* (2015) studied rainfall and hydrological droughts in the high basin of the river Senegal; Sarr *et al.* (2015) examined inter-annual variations of the annual mean precipitation, the annual standard deviation of daily precipitation, the frequency of wet days, the maximum number of consecutive dry days, the maximum three-day rainfall total, the wet day precipitation intensity and the 90th per centile of rain-day precipitation using daily precipitation data from thirty one Senegalese stations spanning the period from 1950 to 2007; Wade *et al.* (2015) studied spatial coherence of rainfall over the Saloum delta in Senegal from seasonal to decadal time scales; Bodian *et al.* (2016a) performed rainfall-runoff modelling of water resources in the upper Senegal River basin; Bodian *et al.* (2016b) evaluated the capacity of Tropical Rainfall Measuring Mission satellite data to simulate the observed runoffs over the Bafing, the main important tributary of the Senegal River; Bodian *et al.* (2016c) analysed, for the Senegal River basin, the evolution of four classes of daily precipitation, the number of rainy days and the duration of the rainy season; Cisse *et al.* (2016) studied the impact of rainfall intra-seasonal variability on vegetation growth in the Ferlo basin, Senegal; Sambou *et al.* (2018) studied the spatial and temporal rainfall variability of the transboundary catchment area of Kayanga/Geba River between the Republic of Guinea, Senegal and Guinea-Bissau; Nouaceur and Murarescu (2020) provided trend analysis of rainfall variability in West Africa, including Senegal, Mauritania and Burkina Faso; Gebremichael *et al.* (2022) produced medium-range precipitation forecasts in the Senegal River basin.

The contents of the paper are organized as follows. Section 2 describes the data from twelve locations in Senegal: Dakar, Capskiring, Dioubel, Kolda, Kedougou, Zinguinchor, Saintlouis, Matam, Tambacounda, Linguere, Podor and Kaolack. Section 3 describes the method used to analyze the data. Section 4 presents the results of the method and their discussion. The paper is concluded in Section 5.

2. Data

The data are monthly rainfall in millimetres from 2002 to 2021 for twelve stations in Senegal. The station names and years of record are given in Table 1. The

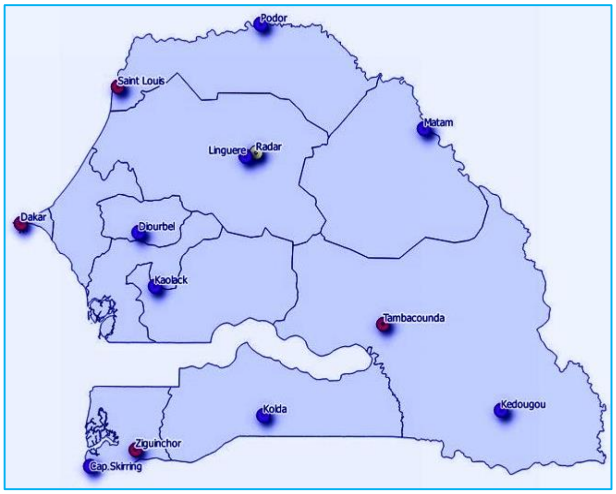

Fig. 1. Locations of the twelve stations

locations of the stations are shown in Fig. 1. We see that the stations give a good representation of the geography of Senegal. The data were obtained from the Department of Meteorology in Dakar.

The monthly maximum rainfall for each year was recorded as the maximum of the twelve monthly values. Some summary statistics (mean, median, skewness, kurtosis, standard deviation, range, minimum and maximum) of the monthly maximum rainfall are also shown in Table 1.

The largest monthly maximum rainfall is between 290.81 mm and 1106.11 mm. Capskiring has the most abundant monthly maximum rainfall. Podor has the least abundant monthly maximum rainfall. The smallest monthly maximum rainfall is 1 mm. The mean values in all the locations are smaller than their median values, which indicates that the rainfall data are positively skewed. This is confirmed by the positive values of skewness. The kurtosis values for all but two of the locations are less than 3, which indicates that their distributions are lighter than the normal distribution. The kurtosis values for Diourbel and Kaolack are larger than 3, which indicates that their distributions are heavier than the normal distribution. Ziguinchor has the largest standard deviation with a value of 180.69 mm. Dakar has the smallest standard deviation. Dakar has the largest coefficient of variation with a value of 80.07. Kedougou has the smallest coefficient of variation.

3. Method

Let X denote a random variable representing the monthly maximum rainfall. According to extreme value theory [Leadbetter *et al.* (1983); Resnick (1987) and Embrechts *et al.* (1997)], the cumulative distribution function of X can be approximated by :

$$F_x(x) = \exp\left[-\left(1+\xi\frac{x-\mu}{\sigma}\right)^{-1/\xi}\right] \qquad (1)$$

for $\mu - \sigma/\xi \le x < \infty$ if $\xi > 0$, $-\infty < x < \infty$ if $\xi = 0$ and $-\infty < x \le \mu - \sigma/\xi$ if $\xi < 0$, where $-\infty < \mu < \infty$ denotes a location parameter, $\sigma > 0$ denotes a scale parameter and $-\infty < \xi < \infty$ denotes a shape parameter. Note that if $\xi > 0$ then X has a heavy tail bounded below by $\mu - \sigma/\xi$. If $\xi < 0$ then X has a short tail bounded above by $\mu - \sigma/\xi$.

The distribution in (1) is known as the Generalized Extreme Value (GEV) distribution. The GEV distribution was fitted to the data in Section 2 by the method of maximum likelihood. Suppose $x_1, x_2, \ldots, x_n$ is an enumeration of the data in Section 2. The maximum likelihood estimates of μ, σ and ξ were obtained by maximizing :

$$L(\mu,\sigma,\xi) = \frac{1}{\sigma^n}\Pi_{i=1}^{n} \left\{\left[1+\xi\frac{x_i-\mu}{\sigma}\right]^{-\frac{1}{\xi}-1}\exp\left[-\left(1+\xi\frac{x_i-\mu}{\sigma}\right)^{-\frac{1}{\xi}}\right]\right\}$$

over all possible values of μ, σ and ξ. The maximum likelihood estimates are the values of μ, σ and ξ corresponding to the maximum of $L(\mu, \sigma, \xi)$. The maximization was performed using the command fgev in the R package evd (Stephenson, 2018; R. Core Team, 2022). Other distributions (for example, the normal distribution) may provide better fits to the monthly maximum temperature. But the GEV distribution is theoretically justified.

The GEV distribution has been used to model extreme rainfall from many locations around the world. We mention Athens, Greece (Koutsoyiannis and Baloutsos, 2000), Malaysia (Zalina *et al.*, 2002), Ukraine, Moldova and Romania (Villarini, 2012), India (Srivastava *et al.*, 2016), north of Iran (Modarres *et al.*, 2018), northwestern Algeria (Boucefiane and Meddi, 2019), Mumbai, India (Parchure and Gedam, 2019), South Africa (Diriba and Debusho, 2021) and Somalia (Mohamed and Adam, 2022).

Let $\hat{\mu}$, $\hat{\sigma}$ and $\hat{\xi}$ denote the maximum likelihood estimates of μ, σ and ξ, respectively. A quantity of interest based on (1) is the T-year return level loosely interpreted

TABLE 2

Estimates, standard errors and 95 per cent confidence intervals for the parameters of the GEV distribution for monthly maximum rainfall

		ξ	σ	μ
Capskiring	Parameter estimates	0.003	141.6	397.7
	Standard errors	0.109	23.562	0.113
	Confidence interval (95%)	(-0.219, 0.225)	(95.409, 187.771)	(330.053,465.305)
Dakar	Parameter estimates	0.253	68.006	182.798
	Standard errors	0.32	16.69	19.80
	Confidence interval (95%)	(-0.374,0.880)	(35.286,100.725)	(143.992,221.604)
Diourbel	Parameter estimates	-0.420	106.457	206.857
	Standard errors	0.114	19.647	0.149
	Confidence interval (95%)	(-0.713, -0.128)	(67.949,144.965)	(154.443,259.271)
Kaolack	Parameter estimates	-0.011	84.062	260.660
	Standard errors	22.285	17.325	0.227
	Confidence interval (95%)	(-0.350,0.538)	(50.106, 118.017)	(216.983, 304.338)
Kedougou	Parameter estimates	-0.433	113.576	284.345
	Standard errors	0.11	18.87	27.35
	Confidence interval (95%)	(-0.648, -0.217)	(76.597,150.555)	(230.749, 337.942)
Kolda	Parameter estimates	-0.319	164.536	300.239
	Standard errors	0.141	28.270	40.435
	Confidence interval (95%)	(-0.595, -0.042)	(109.127, 219.945)	(220.988, 379.490)
Linguere	Parameter estimates	0.118	78.272	164.128
	Standard errors	0.220	15.966	0.220
	Confidence interval (95%)	(-0.313,0.549)	(46.980,109.565)	(123.775,204.481)
Matam	Parameter estimates	0.393	66.048	170.161
	Standard errors	0.230	15.456	17.126
	Confidence interval (95%)	(-0.057,0.844)	(35.754, 96.342)	(136.596, 203.726)
Podor	Parameter estimates	-0.074	57.840	101.596
	Standard errors	14.634	10.478	0.174
	Confidence interval (95%)	(-0.414, 0.267)	(37.303, 78.376)	(72.914,130.277)
Saintlouis	Parameter estimates	0.217	46.541	131.592
	Standard errors	0.246	10.244	12.520
	Confidence interval (95%)	(-0.266,0.700)	(26.463, 66.619)	(107.0524, 156.132)
Tambacounda	Parameter estimates	0.042	80.856	244.544
	Standard errors	0.153	14.221	0.134
	Confidence interval (95%)	(-0.220,0.305)	(52.981,108.730)	(205.619,283.470)
Ziguinchor	Parameter estimates	437.026	144.639	437.026
	Standard errors	0.200	27.159	37.357
	Confidence interval (95%)	(-0.540,0.245)	(91.409,197.868)	(363.807,510.245)

as the monthly maximum rainfall expected on average once in every T years. Let x_T denote the T-year return level corresponding to (1). It must satisfy :

$$F_x(x_T) = 1 - \frac{1}{T^{\bullet}} \qquad (2)$$

Inverting (2), we obtain

$$x_T = \hat{\mu} + \frac{\hat{\sigma}}{\hat{\xi}}\left\{\left[-\log\left(1-\frac{1}{T}\right)\right]^{-\hat{\xi}} - 1\right\} \qquad (3)$$

See equation (3.4) in Coles (2001).

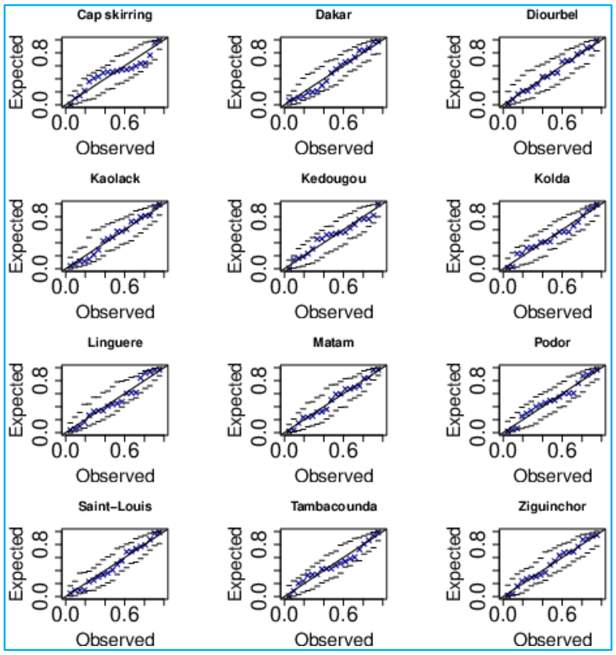

Fig. 2. Observed probabilities versus expected probabilities (plotted as dots) for the fit of the GEV distribution for monthly maximum rainfall from the locations. The diagonal lines correspond to the equality of probabilities. The dashed lines are 95 per cent simulated confidence intervals

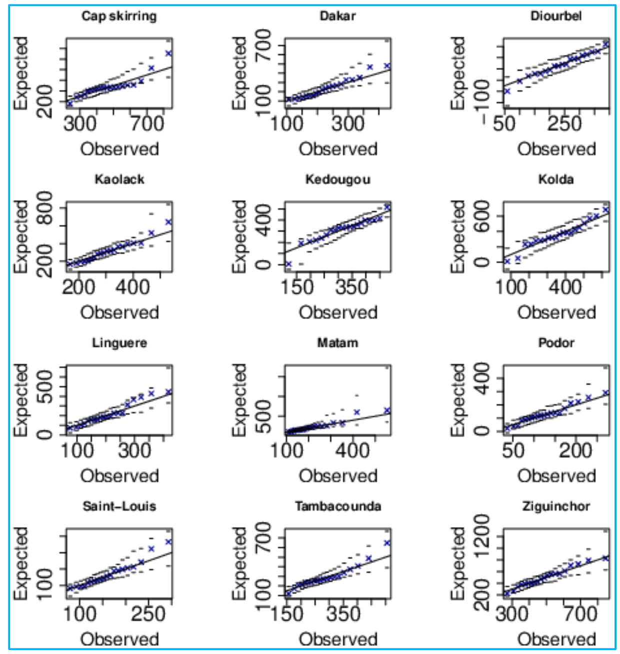

Fig. 3. Observed quantiles versus expected quantiles (plotted as dots) for the fit of the GEV distribution for monthly maximum rainfall from the locations. The diagonal lines correspond to the equality of quantiles. The dashed lines are 95 per cent simulated confidence intervals

4. Results and discussion

The GEV distribution was fitted to the monthly maximum rainfall data from each of the twelve stations. The estimates, standard errors and 95 per cent confidence intervals for the parameters of the GEV distribution are shown in Table 2.

The shape parameter estimate is not significantly different from zero for Capskiring, Dakar, Kaolack, Linguere, Matam, Podor, Saintlouis, Tambacounda and Ziguinchor. The shape parameter estimate is significantly negative for Diourbel, Kedougou and Kolda. The monthly maximum rainfall is bounded above by the probable maximum, $\hat{\mu}-\hat{\sigma}/\hat{\xi}$, for these three locations. $\hat{\mu}-\hat{\sigma}/\hat{\xi}$ takes the values 460.1 mm, 546.8 mm and 816.0 mm for Diourbel, Kedougou and Kolda, respectively. The largest of the probable maximum of monthly maximum rainfall is for Kolda. The smallest is for Diourbel.

Ziguinchor gives the largest of the estimates for the scale and location parameters. Saintlouis gives the smallest of the estimates for the scale parameter. Podor gives the smallest of the estimates for the location parameter. So, the extreme rainfall is most variable for Ziguinchor.

Capskiring gives the smallest of the standard errors for the shape and location parameter estimates. Kolda gives the largest of the standard errors for the scale and location parameter estimates. Kaolack gives the largest of the standard errors for the shape parameter estimate. Saintlouis gives the smallest of the standard errors for the scale parameter estimate. So, Capskiring and Saintlouis give the most accurate of the parameter estimates. Kolda and Kaolack give the least accurate of the parameter estimates.

The fit of the GEV distribution for each station was checked by probability and quantile plots. The plots are shown in Figs. 2 and 3 for the twelve stations.

Probability plots are plots of $\hat{F}\left[x_{(i)}\right]$, the observed probabilities, versus i / (n + 1), the expected probabilities, where $x_{(1)} \leq x_{(2)} \leq \ldots x_{(n)}$ are the data arranged in increasing order and $\hat{F}(x)=\exp\left[-\left(1+\hat{\xi}\frac{x-\hat{\mu}}{\hat{\sigma}}\right)^{-\frac{1}{\hat{\xi}}}\right]$.

Quantile plots are plots of $x_{(i)}$, the observed quantiles, versus $\hat{F}^{-1}\left[i/(n+1)\right]$, the expected quantiles, where, $\hat{F}^{-1}(\cdot)$ denotes the inverse function of $\hat{F}(\cdot)$. The diagonal straight lines in Fig. 2 correspond to the observed and expected probabilities being equal. The diagonal straight lines in Fig. 3 correspond to the observed and expected quantiles being equal. The dashed lines in Figs. 2 and 3 are the 95 per cent simulated confidence intervals. The confidence intervals in Fig. 2 were computed as follows:

(*i*) simulate a random sample of size *n* from $\hat{F}$;

(*ii*) refit the GEV distribution to the sample and let $\tilde{\mu}$, $\tilde{\sigma}$ and $\tilde{\xi}$ denote the parameter estimates;

(*iii*) compute $\tilde{F}\left[x_{(i)}\right] = \exp\left[-\left(1+\tilde{\xi}\,\frac{x_{(i)}-\tilde{\mu}}{\tilde{\sigma}}\right)^{-\frac{1}{\tilde{\xi}}}\right]$ for $i = 1, 2, \ldots, n$;

(*iv*) repeat steps (*i*)-(*iii*) 10000 times, giving 10000 values for $\tilde{F}\left[x_{(i)}\right]$;

(*v*) compute the empirical distribution function of the 10000 values in step (iv), denoting it by $\hat{\tilde{F}}$;

(*vi*) compute $\hat{\tilde{F}}^{-1}(0.025)$ and $\hat{\tilde{F}}^{-1}(0.725)$, where $\hat{\tilde{F}}^{-1}(\cdot)$ denotes the inverse function of $\hat{\tilde{F}}(\cdot)$;

(*vii*) plot $\left[\hat{\tilde{F}}^{-1}(0.025), \hat{\tilde{F}}^{-1}(0.725)\right]$, the 95 per cent simulated confidence interval, versus *i* / (*n* + 1) for $i = 1, 2, \ldots, n$.

The confidence intervals in Fig. 3 were computed as follows:

(*i*) simulate a random sample of size *n* from $\hat{F}$;

(*ii*) refit the GEV distribution to the sample and let $\tilde{\mu}, \tilde{\sigma}$ and $\tilde{\xi}$ denote the parameter estimates;

(*iii*) compute $\tilde{F}^{-1}[i/(n+1)]$ for $i = 1, 2, \ldots, n$, where $\tilde{F}^{-1}(\cdot)$ denotes the inverse function of (4);

(*iv*) repeat steps (i)-iii) 10000 times, giving 10000 values for $\tilde{F}^{-1}[i/(n+1)]$;

(*v*) compute the empirical distribution function of the 10000 values in step (*iv*), denoting it by $\hat{\tilde{F}}$;

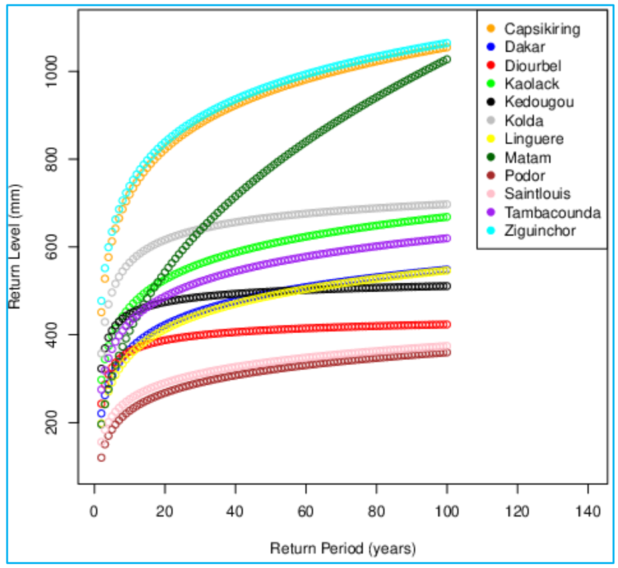

Fig. 4. Estimates of x_T versus $T = 2, 3, \ldots, 100$

(*vi*) compute $\hat{\tilde{F}}^{-1}(0.025)$ and $\hat{\tilde{F}}^{-1}(0.725)$, where $\tilde{F}^{-1}(\cdot)$ denotes the inverse function of $\hat{\tilde{F}}(\cdot)$;

(*vii*) plot $\left[\hat{\tilde{F}}^{-1}(0.025), \hat{\tilde{F}}^{-1}(0.725)\right]$, the 95 per cent simulated confidence interval, versus $x_{(i)}$ fir $i = 1, 2 \ldots, n$.

The closer the plotted points (in Figs. 2 and 3) are to the diagonal lines the better the fit. The plotted points must lie within the simulated confidence intervals for the fit to be considered adequate. Hence, the fit of the GEV distribution for monthly maximum rainfall from the twelve locations is adequate.

In addition to using probability and quantile plots, we tested goodness of fit using the Kolmogorov-Smirnov, Anderson-Darling and Cramer-von Mises tests. The Kolmogorov-Smirnov test gave the *p*-values of 0.129, 0.169, 0.099, 0.093, 0.164, 0.051, 0.129, 0.133, 0.111, 0.128, 0.150 and 0.185 for the twelve locations. The Anderson-Darling test gave the *p*-values of 0.184, 0.124, 0.060, 0.060, 0.096, 0.129, 0.068, 0.101, 0.087, 0.080, 0.125 and 0.140. The Cramer-von Mises test gave the *p*-values of 0.180, 0.064, 0.057, 0.120, 0.142, 0.193, 0.141, 0.071, 0.078, 0.073, 0.053 and 0.179.

Having checked the goodness of fit, we computed (3) for every station and a range of values of *T*. Plots of x_T for $T = 2, \ldots, 1000$ are shown in Fig. 4.

As expected, the return level estimates increase with the return period. For all return periods greater than 50, the return level estimates are largest for Ziguinchor,

TABLE 3

Stations exhibiting significant trends in the location parameter

Station	Trend	$\hat{a}$ (se)	$\hat{b}$ (se)	p-value
Diourbel	Positive	113.916 (39.367)	10.574 (3.129)	0.001
Kedougou	Positive	200.262 (25.712)	10.963 (0.177)	0.000
Linguere	Positive	105.07 (32.193)	6.63 (2.684)	0.018
Tambacounda	Positive	192.913 (29.583)	5.302 (2.334)	0.024

second largest for Capskiring, third largest for Matam, fourth largest for Kolda, fifth largest for Kaolack, sixth largest for Tambacounda, seventh largest for Dakar, eighth largest for Linguere, ninth largest for Kedougou, tenth largest for Diourbel and eleventh largest for Saintlouis. The return level estimates are smallest for Podor. These findings are consistent with the contour of rainfall given in Fall *et al.* (2006a) and the contour of maximum three-day total rainfall given in Fig. 3 of Sarr *et al.* (2015).

Matam has the most peaked of the return level estimates. Ziguinchor and Capskiring have the second most peaked of the return level estimates. The other stations have more or less the same amount of peakedness.

Finally, we investigated to see if there are significant trends in the monthly maximum rainfall for each station. We fitted (1) with the location parameter $\mu = a + b \times (\text{year} - 2001)$, where b is the trend parameter. By comparing the fit of this model with the earlier fit of the GEV distribution, we can see if the trend is significant or not. We also fitted models like $\mu = a + b \times (\text{year} - 2001) + c \times (\text{year} - 2001)^2$ and $\mu = \exp[a + b \times (\text{year} - 2001)]$, but they did not provide significantly better fits. The methodology used for fitting models like $\mu = a + b \times (\text{year} - 2001)$ is described in Chapter 6 of Coles (2001).

Table 3 lists the station names and the parameter estimates of a and b and p-values showing significance of the trend. We see that only four of the stations exhibit significant trends. All four stations exhibit positive trends. These trends may be due to climate change or other factors.

5. Conclusions

This paper has provided the first statistical analysis of maximum rainfall in Senegal involving data from twelve stations. The generalized extreme value distribution was shown to provide an adequate fit (as assessed by probability plots, quantile plots and goodness of fit tests) to data from each station.

The wettest areas with respect to return levels are Ziguinchor, Capskiring and Matam. The driest areas with respect to return levels are Diourbel, Saintlouis and Podor. Four of the stations (Diourbel, Kedougou, Linguere and Tambacounda) exhibit significant positive trends in maximum rainfall. The remaining stations do not exhibit significant trends.

The results presented in this paper can inform positive actions by the Government of Senegal: for example, further vegetables and other commodities less reliable on rain can be planted on the driest areas; increased agricultural and electricity production based on water can take place in the wettest areas; increased electricity production based on solar energy can take place in the driest areas; and so on.

Future work are to use techniques such as spatial temporal modeling, Bayesian methods, entropy based methods, regional analysis based on L moments, bootstrapping methods, genetic programming methods, nonparametric copulas, time varying copulas, quantile regression methods, max-stable processes, neural networks, artificial intelligence methods, wavelet transformation analysis, vector generalized additive models and the generalized Pareto distribution for modeling maximum rainfall in Senegal.

Acknowledgments

The authors would like to thank the Editor and the referee for careful reading and comments which greatly improved the paper.

Disclaimer : The contents and views expressed in this study are the views of the authors and do not necessarily reflect the views of the organizations they belong to.

References

Bodian, A., Dezetter, A. and Dacosta, H., 2016a, "Rainfall-runoff modelling of water resources in the upper Senegal River basin", *International Journal of Water Resources Development*, **32**, 89-101.

Bodian, A., Dezetter, A., Deme, A. and Diop, L., 2016b, "Hydrological evaluation of TRMM rainfall over the Upper Senegal River basin", *Hydrology*, 3, article number 15.

Bodian, A., Ndiaye, O. and Dacosta, H., 2016c, "Variability of daily rainfall characteristics over the Senegal River basin : Before and after the abrupt rainfall change", *Hydrological Sciences Journal*, **61**, 905-913.

Boucefiane, A. and Meddi, M., 2019, "Regional growth curves and extreme precipitation events estimation in the steppe area of northwestern Algeria", *Atmosfera*, **32**, 287-303.

Camberlin, P. and Diop, M., 2003, "Application of daily rainfall principal component analysis to the assessment of the rainy season characteristics in Senegal", *Climate Research*, **23**, 159-169.

Cisse, S., Eymard, L., Ottle, C., Ndione, J. A., Gaye, A. T. and Pinsard, F., 2016, "Rainfall intra-seasonal variability and vegetation growth in the Ferlo basin (Senegal)", *Remote Sensing*, 8, article number 66.

Coles, S. G., 2001, "An introduction to statistical modeling of extreme values", *Springer Verlag*, New York.

Diriba, T. A. and Debusho, L. K., 2021, "Statistical modeling of spatial extremes through max-stable process models : Application to extreme rainfall events in South Africa", *Journal of Hydrologic Engineering*, **26**, article number 05021028.

Embrechts, P., Klüppelberg, C. and Mikosch, T., 1997, "Modelling extremal events for insurance and finance", *Springer Verlag*, Berlin.

Fall, S., Niyogi, D. and Semazzi, F. H. M., 2006a, "Analysis of mean climate conditions in Senegal (1971-98)", *Earth Interactions*, **10**, article number 5.

Fall, S., Semazzi, F. H. M., Dutta, D., Niyogi, S., Anyah, R. O. and Bowden, J., 2006b," The spatiotemporal climate variability over Senegal and its relationship to global climate", *International Journal of Climatology*, **26**, 2057-2076.

Faye, C., Sow, A. A. and Ndong, J. B., 2015, "Study of rainfall and hydrological droughts in tropical Africa : Characterization and mapping of drought indices in the high basin of the river Senegal", *Physio-Geo*, **9**. doi : 10.4000/physio-geo.4388.

Gebremichael, M., Yue, H. W., Nourani, V. and Damoah, R., 2022, "The skills of medium-range precipitation forecasts in the Senegal River basin", *Sustainability*, **14**, article number 3349.

Kakane, V. C. K. and Imbernon, J., 1992, "Estimation of rainfall in Senegal using the satellite NOAA-9/AVHRR", *International Journal of Remote Sensing*, **13**, 2059-2068.

Koutsoyiannis, D. and Baloutsos, G., 2000, "Analysis of a long record of annual maximum rainfall in Athens, Greece and design rainfall inferences", *Natural Hazards*, **22**, 29-48.

Leadbetter, M. R., Lindgren, G. and Rootzén, H., 1983, "Extremes and related properties of random sequences and processes", *Springer Verlag*, New York.

Modarres, R., Ghadami, M., Naderi, S. and Naderi, M., 2018, "Future extreme rainfall change projections in the north of Iran", *Meteorological Applications*, **25**, 40-48.

Mohamed, J. and Adam, M. B., 2022, "Modeling of magnitude and frequency of extreme rainfall in Somalia", *Modeling Earth Systems and Environment*, doi : 10.1007/s40808-022-01363-0.

Moron, V., Robertson, A. W. and Ward, M. N., 2006, "Seasonal predictability and spatial coherence of rainfall characteristics in the tropical setting of Senegal", *Monthly Weather Review*, **134**, 3248-3262.

Moron, V., Robertson, A. W., Ward, M. N. and Ndiaye, O., 2008a, "Weather types and rainfall over Senegal, part I : Observational analysis", *Journal of Climate*, **21**, 266-287.

Moron, V., Robertson, A. W., Ward, M. N. and Ndiaye, O., 2008b, "Weather types and rainfall over Senegal. part II: Downscaling of GCM simulations", *Journal of Climate*, **21**, 288-307.

Ndour, P., Kane, A., Fall, A. N. and Lazar, G., 2012, "Rainfall variability in senegalese rural area: Implications on water resources in the borough of Fimela", *Environmental Engineering and Management Journal*, **11**, 2239-2247.

Negre, T., Imbernon, J., Guinot, J. P., Seguin, B., Berges, J. C. and Guillot, B., 1988, "Rainfall estimation and monitoring in Senegal by cumulation of the thermal infrared images of the Meteosat satellite", *Agronomie Tropicale*, **43**, 279-288.

Nouaceur, Z. and Murarescu, O., 2020, "Rainfall variability and trend analysis of rainfall in West Africa (Senegal, Mauritania, Burkina Faso)", *Water*, **12**, article number 1754.

Nzeukou, A. and Sauvageot, H., 2002, "Distribution of rainfall parameters near the coasts of France and Senegal", *Journal of Applied Meteorology*, **41**, 69-82.

Parchure, A. S. and Gedam, S. K., 2019, "Probability distribution analysis of extreme rainfall events in a flood-prone region of Mumbai, India", *Arabian Journal of Geosciences*, **12**, article number 369.

R. Core Team, 2022, "R : A language and environment for statistical computing. R Foundation for Statistical Computing",, *Vienna*, Austria.

Resnick, S. I., 1987, "Extreme values, regular variation and point processes", *Springer Verlag*, New York.

Rust, H. W., Vrac, M., Sultan, B. and Lengaigne, M., 2013, "Mapping weather-type influence on Senegal precipitation based on a spatial-temporal statistical model", *Journal of Climate*, **26**, 8189-8209.

Sambou, S., 2004, "Frequency analysis of daily rainfall in the Sahelian area: Case of the upstream basin of the Senegal River", *Hydrological Sciences Journal*, **49**, 115-129.

Sambou, S., Dacosta, H. and Paturel, J. E., 2018, "Spatio-temporal variability of rainfall from 1932 till 2014 in the Kayanga/Geba River watershed (Republic of Guinea, Senegal, Guinea-Bissau)", *Physio-Geo*, **12**, 61-78.

Sarr, M. A., Gachon, P., Seidou, O., Bryant, C. R., Ndione, J. A. and Comby, J., 2015, "Inconsistent linear trends in Senegalese rainfall indices from 1950 to 2007", *Hydrological Sciences Journal*, **60**, 1538-1549.

Srivastava, A. K., Singh, G. P. and Singh, O. P., 2016, "Variability and trends in extreme rainfall over India", *MAUSAM*, **67**, 745-766.

Stephenson, A., 2018, "evd: Functions for extreme value distributions", R. package version 2.3-3.

Thiam, E. H. I. and Singh, V. P., 2002, "Space-time-frequency analysis of rainfall, runoff and temperature in the Casamance River basin, southern Senegal, West Africa", *Water SA*, **28**, 259-270.

Villarini, G., 2012, "Analyses of annual and seasonal maximum daily rainfall accumulations for Ukraine, Moldova and Romania", *International Journal of Climatology*, **32**, 2213-2226.

Wade, M., Mignot, J., Lazar, A., Gaye, A. T. and Carre, M., 2015, "On the spatial coherence of rainfall over the Saloum delta (Senegal) from seasonal to decadal time scales", *Frontiers in Earth Science*, **3**, article number 30.

Zalina, M. D., Desa, M. N. M., Nguyen, V. T. V. and Kassim, A. H. M., 2002, "Selecting a probability distribution for extreme rainfall series in Malaysia", *Water Science and Technology*, **45**, 63-68.